Supporting Information

Insulation board-derived N/O self-doped porous carbon as electrode materials for high-performance symmetric supercapacitor

Yingjie Su[#], Zhenjie Lu[#], Junxia Cheng, Xuefei Zhao, Xingxing Chen[*], Lijuan Gao[*]

School of Chemical Engineering, University of Science and Technology Liaoning, Qianshan Middle Road 185, 114051 Anshan, China

[#] *The two authors contributed equally.*

[*] *Corresponding authors. E-mail: gaolijuan@ustl.edu.cn, xingchenstar79@163.com (X. X. Chen).*

Experimental

In a three-electrode system, the specific capacitance (C, F g^{-1}) obtained from the galvanostatic charging/discharging (GCD) curves was calculated according to the formula:

$C=(I\Delta t)/(m\Delta V)$,

where I, Δt, m and ΔV represent discharge current (A), discharge time (s), electrode mass (g) and discharge voltage (V), respectively [1].

For the symmetrical supercapacitor, the specific capacitance (C$_s$, F g^{-1}) calculated from the GCD curves was according to formula:
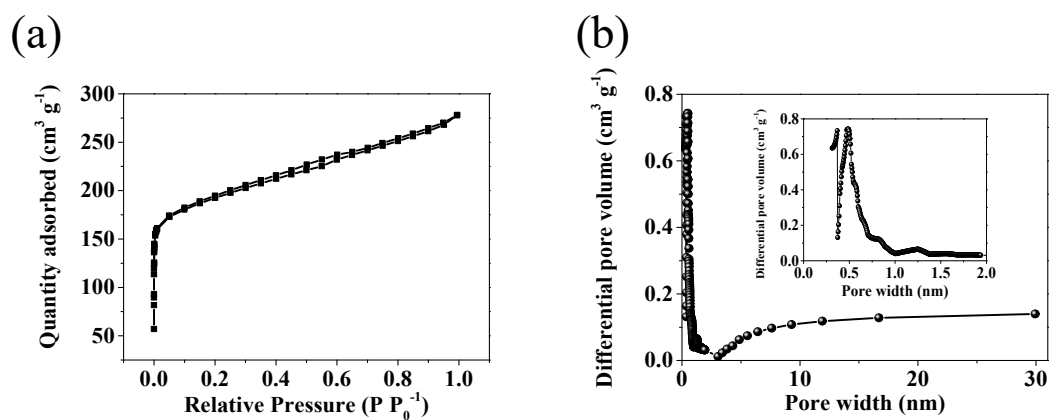
$C_s=(2I\Delta t)/(m\Delta V)$,

where I, Δt, m and ΔV represent discharge current (A), discharge time (s), electrode mass (g) and cell-operation discharge voltage (V), respectively [2].
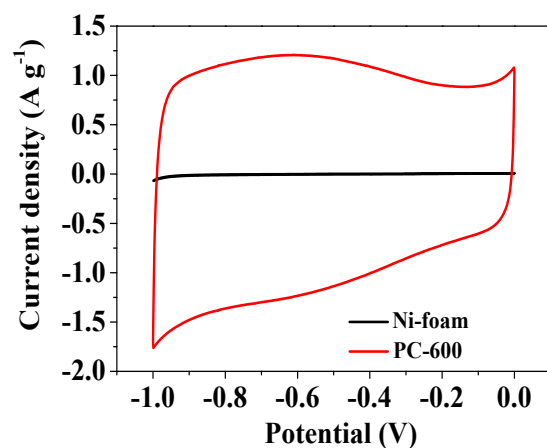
The energy density (E, Wh kg^{-1}) and power density (P, W kg^{-1}) were respectively calculated with the equations of $E=0.5C_sV^2/3.6$ and $P=3600E/\Delta t$ [3,4].
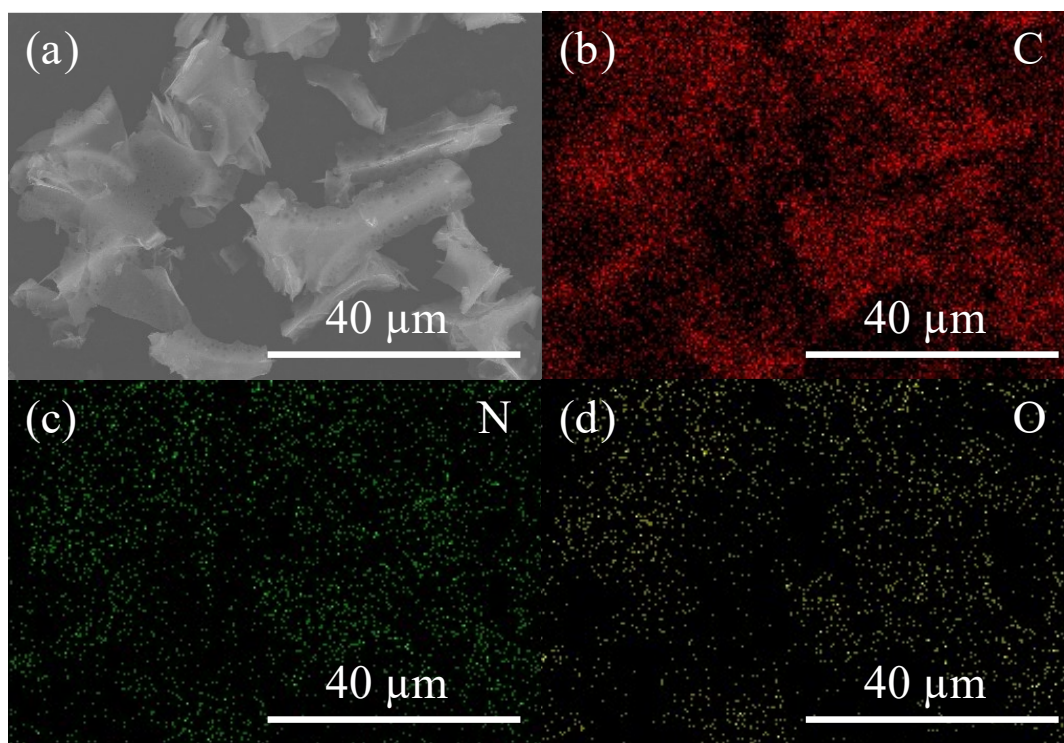
Figure S1 (a) SEM image of PC-600 and its corresponding elemental mappings of (b) C, (c) N, and (d) O.
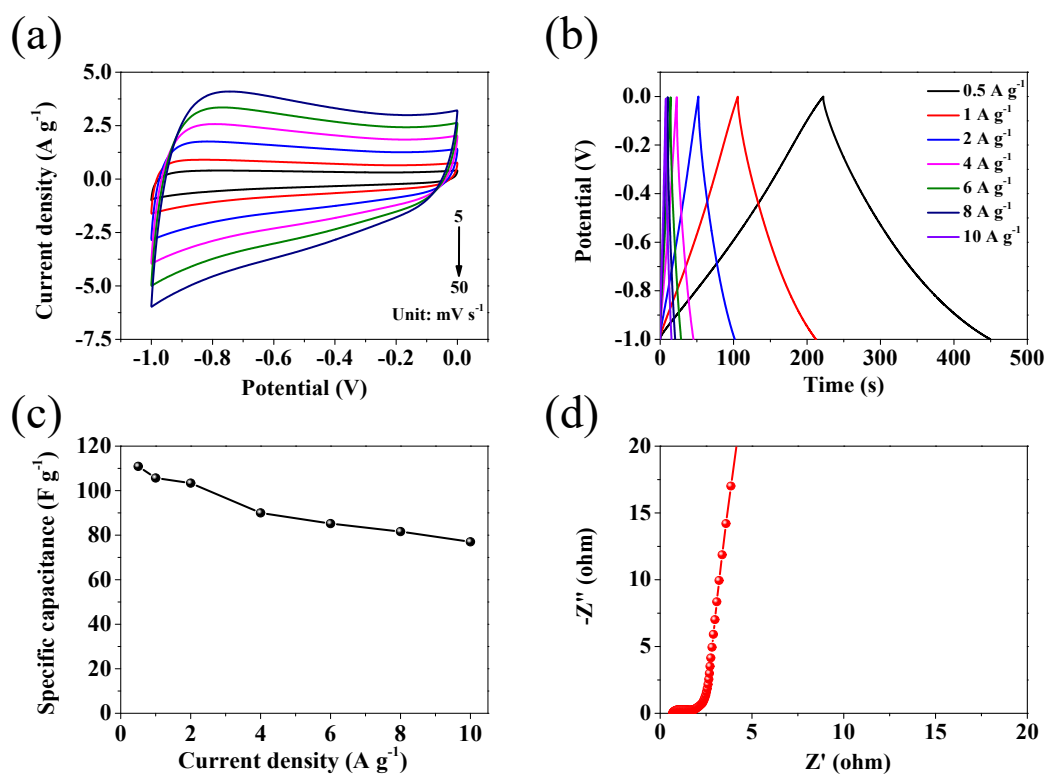

Figure S2 (a) N$_2$ adsorption-desorption isotherms, (b) and (inset) pore size distribution curves of CC.

Figure S3 The comparison of CV curves of pure Ni-foam and PC-600 loaded on Ni-foam (Scan rate: 5 mV s^{-1}).

Figure S4 (a) CV, (b) GCD, (c) specific capacitance at different current densities and (d) EIS curves of CC.
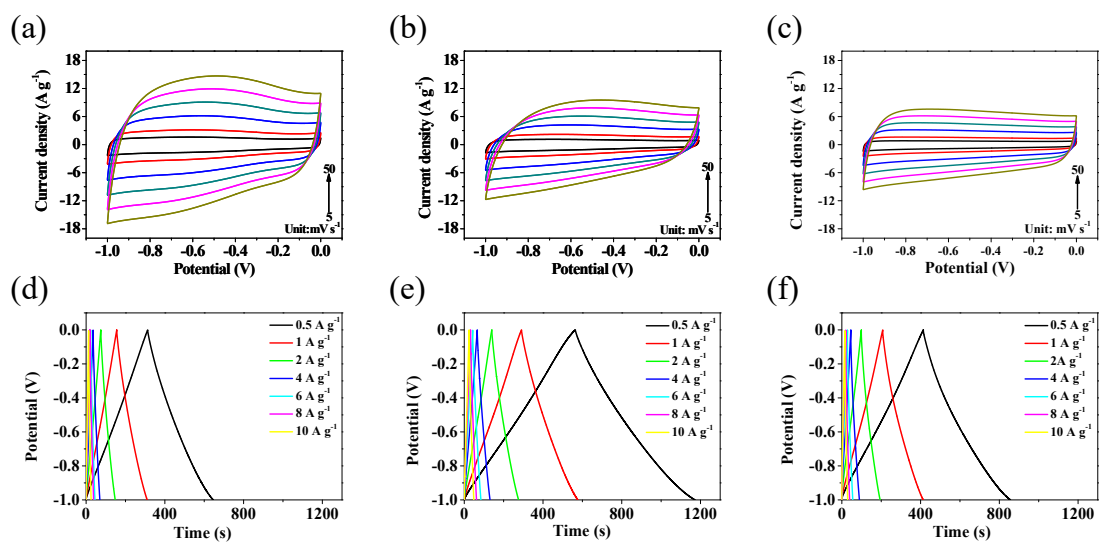
Figure S5 (a~c) CV curves at different scan rates and GCD curves at different current densities of PC-500, PC-700 and PC-800.

Figure S6 (a) Bode plot,(b)real and (c) imaginary parts of specific capacitance fitted by EIS.

Table S1 Nitrogen adsorption-desorption measurements at 77 k for CC, PC-500, PC-600, PC-700 and PC-800.

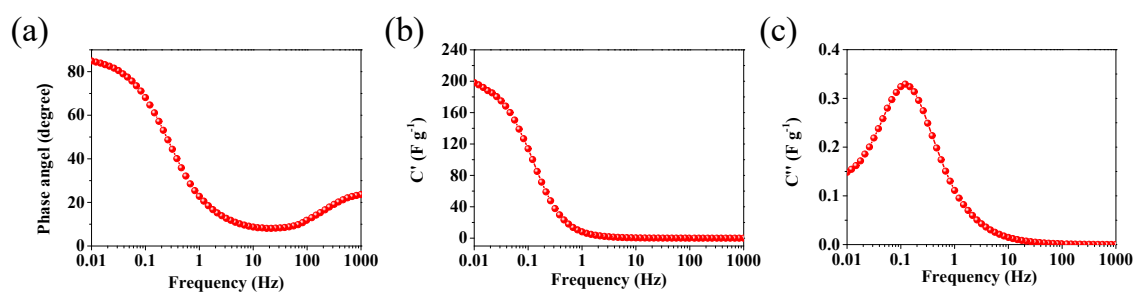| Sample	S_{BET} $(m^2\ g^{-1})$	V_{tot} $(cm^3\ g)$	V_{mic} $(cm^3\ g^{-1})$	V_{meso} $(cm^3\ g^{-1})$	D_{pore} (nm)
CC	98	0.430	0.289	0.156	1.38
PC-500	145	0.134	0.062	0.091	3.68
PC-600	960	0.413	0.368	0.059	1.72
PC-700	1383	0.605	0.532	0.097	1.74
PC-800	1395	0.648	0.540	0.141	1.86

Table S2 The relative concentrations of nitrogen and oxygen estimated from XPS in PC-500, PC-600, PC-700 and PC-800.

Sample	O 1s				N 1s				
	Total	O-C=O	C=O	C-O-H	Total	N-O	N-Q	N-5	N-6
	O %	%	%	%	N %	%	%	%	%
PC-500	11.43	9.62	78.57	11.81	1.84	20.27	31.28	25.95	22.50
PC-600	12.96	3.43	28.87	67.70	1.61	17.97	39.00	26.88	16.15
PC-700	13.22	10.40	76.01	13.59	0.93	23.61	27.17	26.74	22.48
PC-800	12.05	61.58	31.82	6.60	0.83	21.56	24.55	28.12	25.77

Table S3 The comparison of electrochemical performance of the supercapacitors using waste material-derived porous carbon as the electrodes.

Sample	Specific Capacitance ($F\ g^{-1}$)	Power Density ($W\ kg^{-1}$)	Energy Density ($Wh\ kg^{-1}$)	Stability	Ref.
PC-600	262.2	500	17.4	100% (20000 c)	This work
QPC-3	254	100	9.5	93% (10000 c)	[5]
U-3DHPC	284.1	200.7	19.2	86.5% (10000 c)	[6]
HPCR-800	48.7	100	6.77	81% (10000 c)	[7]
TC-1	356.4	300	10.4	92.8% (5000 c)	[8]
HPC-4	452.7	140	14.1	90% (6000 c)	[9]
WB-HPC-700	413	220.9	22.3	93% (10000 c)	[10]

Reference

[1] C. Ma, L.Q. Wu, M. Dirican, H. Cheng, J.J. Li, Y. Song, J.L. Shi, X.W. Zhang, Carbon black-based porous sub-micron carbon fibers for flexible supercapacitors, Appl. Surf. Sci. 537 (2021) 147914.

[2] Y.B. Liu, G.X. Huang, Y.Y. Yuan, Y.H. Yao, Q.R. Liu, B.L. Xing, J.B. Jia, C.X. Zhang, Structural evolution of porous graphitic carbon nanosheets based on quinonyl decomposition for supercapacitor electrodes, Appl. Surf. Sci. 573 (2021) 147824.

[3] J.Q. Cui, J. Yin, J.S. Meng, Y. Liu, M.Y. Liao, T. Wu, M. Dresselhaus, Y.M. Xie, J.H. Wu, C.Z. Lu, X.C. Zhang, Supermolecule cucurbituril subnanoporous carbon supercapacitor (SCSCS), Nano Lett. 21 (2021) 2156－2164.

[4] Y.Y. Tan, D.L. Wu, T. Wang, P.G. Liu, J. Guo, D.Z. Jia, Facile synthesis of functionalized graphene hydrogel for high performance supercapacitor with high volumetric capacitance and ultralong cycling stability, Appl. Surf. Sci. 455 (2018) 683–695.

[5] Y. Sun, J. J. Xue, S.Y. Dong, Y.D. Zhang, Y.F. An, B. Ding, T.F. Zhang, H. Dou, X.G. Zhang, Biomass-derived porous carbon electrodes for high-performance supercapacitors, J. Mater. Sci. 55, (2020) 5166−5176.

[6] C.D. Ma, J.K. Min, J. Gong, X.G. Liu, X.Y. Mu, X.C. Chen, T. Tang, Transforming polystyrene waste into 3D hierarchically porous carbon for highperformance supercapacitors, 253 (2020) 126775.

[7] L. Fang, Y.P. Xie, Y.Y. Wang, Z.W. Zhang, P.F. Liu, N. Cheng, J.F. Liu, Y.C. Tu, H.B. Zhao, J.J. Zhang, Facile synthesis of hierarchical porous carbon nanorods for supercapacitors application, Appl. Surf. Sci. 464 (2019) 479−487.

[8] Z.R. Huang, C.Y. Qin, J. Wang, L. Cao, Z.W. Ma, Q.H. Yuan, Z.D. Lin, P. Zhang, Research on high-value utilization of carbon derived from tobacco waste in supercapacitors, Materials 14 (2021) 1714−1726.

[9] G.Z. Zhao, Y.J. Li, G. Zhu, J.Y. Shi, T. Lu, L.K. Pan, Waste fruit grain orange-derived 3D hierarchically porous carbon for high-performance all-solid-state supercapacitor, Ionics 25 (2019) 3935−3944.

[10] P.F. Yu, Y.R. Liang, H.W. Dong, H. Hu, S.M. Liu, L. Peng, M.T. Zheng, Y. Xiao, Y.L. Liu, Rational synthesis of highly porous carbon from waste bagasse for advanced supercapacitor application, ACS Sustainable Chem. Eng. 6 (2018) 15325−15332.